Available online at www.sciencedirect.com
ScienceDirect
Ceramics International 35 (2009) 725–731
CERAMICS INTERNATIONAL
www.elsevier.com/locate/ceramint

Microstructure and mechanical properties of multi-cation containing α-sialons

Feng Ye *, Chun-Feng Liu, Li-Meng Liu

Institute for Advanced Ceramics, School of Materials Science and Engineering, Harbin Institute of Technology, Harbin 150001, PR China

Received 23 July 2007; received in revised form 17 December 2007; accepted 6 February 2008
Available online 4 June 2008

Abstract

Dense Y-, Yb- and (Y + Yb)-doped α-sialons containing 2 wt.% extra liquid phase were fabricated by hot pressing. The results show that the elongated grains morphology can be obtained by partially substituting Yb with Y as a modifying cation, and hence improve the toughness of the materials. An additional intermediate holding step during sintering has no obvious effect on the microstructures and the mechanical properties. Post-heat treatment can further facilitate the growth of elongated α-sialon grains and increase the toughness of the materials. All the materials exhibited very similar high hardness of over 20 GPa.

Keywords: C. Mechanical properties; D. α-Sialon; Grain morphology; Post-heat treatment

1. Introduction

α-Sialons ($M_xSi_{12-(m+n)}Al_{(m+n)}O_nN_{16-n}$, where M is a metal cation) have attracted intense attention in recent years because of their high hardness, better oxidation resistance, superior creep resistance and the potential to clean up the grain boundary glass-phase compared with β-sialon or other silicon nitrides [1]. These sialons are expected to have wide applications in the near future, particularly for cutting tools or bearing parts. However, their implementation has been limited largely because of their low fracture toughness, which results from an equiaxed grain morphology. Attempts have been made in the past to reinforce α-sialon ceramics with additions of other refractory phases, such as whiskers [2] or particulates [3]. These results show that the increase in toughness is at the expense of hardness of the α-sialons. In order to retain the excellent hardness of the α-sialon matrix, much emphasis has been placed on developing α-sialon ceramics with elongated microstructures.

In recent years, in situ toughened α-sialons have been discovered [4–13], just like an in situ toughened β-sialon, which contain elongated grains and exhibit self-reinforcement. The resulting materials exhibited both strength and toughness of the same order of magnitude as that of β-sialon, with higher apparent hardness. The morphology of α-sialon grains appears to depend on: (a) choice of starting powders [4,7,11]; (b) type of stabilizing cation [4–6,8]; (c) compositions [4,10]; and (d) probably sintering conditions [4,5,7,9,10,13]. Chen and Rosenflanz [4] have emphasized the effect of nucleation rate on the development of elongated α-sialon grains. Their research results indicated that the nucleation and nucleation rate are very important in the formation of elongated α-sialon grains. These workers found that the lower the driving force, the slower the nucleation rate and the higher the probability of forming elongated grain; and that the systematic difference in the microstructures of different rare-earth-stabilized α-sialon ceramics is related to the size of doping cations, i.e. the decreasing tendency to form elongated α-sialon grains with decreasing size of the stabilizing rare-earth cation.

Other results concerning the formation of elongated grains in α-sialon ceramics indicated that the elongated grains were favored by the presence of a liquid phase supersaturated in α-sialon constituents at the sintering temperature [10–13]. The work suggested that the presence of a large amount of liquid

* Corresponding author at: P.O. Box 433, School of Materials Science and Engineering, Harbin Institute of Technology, Harbin 150001, Heilongjiang, PR China. Tel.: +86 451 86414291; fax: +86 451 86414291.
E-mail address: yf306@hit.edu.cn (F. Ye).

0272-8842/$34.00
doi:10.1016/j.ceramint.2008.02.007

phase could promote the formation of elongated α-sialon grains because at the compositions the grains can grow freely in liquid phase. It has also been found that the elongated α-sialon grains could be obtained through post-heat treatment [14]. All these results imply that the elongated α-sialon morphologies can be obtained using suitable composition and firing conditions.

The object of the present work is to explore the effect of mixed modifiers (Y + Yb) on the morphology of α-sialon grains. The influence of sintering condition and post-heat treatment on the microstructure were also investigated.

2. Experimental procedures

α-Sialon phase with the composition of $RE_{0.333}Si_{10}Al_2ON_{15}$ (i.e. $m = 1$ and $n = 1$ in the general formula of α-sialon, $RE_{m/3}Si_{12-(m+n)}Al_{(m+n)}O_nN_{16-n}$, RE = Y and Yb) was selected as the reference composition for investigation. The similar composition $Y_{0.167}Yb_{0.167}Si_{10}Al_2ON_{15}$ was selected for multi-cation α-sialon containing (Y + Yb). For the selected compositions, an excess of 2 wt.% of Y_2O_3, Yb_2O_3 or the mixture of Y_2O_3 and Yb_2O_3 (1:1 mol ratio) were added to achieve full densification. Throughout the work, we will refer to these compositions as Y1010E2, Yb1010E2 and Y/Yb1010E2, respectively. Starting powders were Si_3N_4 (E10 Grade, UBE Industries Ltd., Japan), AlN (Grade F, Tokuyama Corp., Japan), Al_2O_3 (AKP-50, Sumitomo Chemical, Japan), Y_2O_3 (>99.9% purity, Shinetsu Chemical Co., Ltd., Japan) and Yb_2O_3 (>99.9% purity, Shinetsu Chemical Co., Ltd., Japan). When calculating the overall compositions, 2.38 wt.% SiO_2 and 1.83 wt.% Al_2O_3 (according to manufacturer's specifications) on the surface of Si_3N_4 and AlN powders, respectively, were taken into account, and the overall starting compositions are listed in Table 1.

The starting materials were ball-milled with ethanol for 8 h using silicon nitride balls. The powder mixtures were subsequently dried at 40 °C in a rotary evaporator and sieved. The dried powders were hot-pressed (HP) and sintered at 32 MPa under 0.4 MPa nitrogen atmosphere in a graphite resistance furnace. Two different sintering procedures were used. One group of samples was heated directly to 1900 °C and then held there for 1 h. The second group of samples was held at 1500 °C for 1 h before the final HP-sintering step at 1900 °C for 1 h. The heating rate used in both sintering cycles was 30 °C/min. After sintering, the samples were allowed to cool inside the furnace at a cooling rate of about 50 °C/min. Some HP-sintered specimens were also heat-treated at 1900 °C for 1 h in nitrogen atmosphere to further examine the effect of a post-heat treatment on the microstructure.

Table 1
Starting compositions of the investigated α-sialon ceramics (wt.%)

Sample	Si_3N_4	Al_2O_3	AlN	Y_2O_3	Yb_2O_3
Y1010E2	78.00	0.48	13.29	8.22	–
Yb1010E2	74.48	0.47	12.69	–	12.37
Yb/Y1010E2	76.18	0.47	12.98	3.78	6.59

The bulk densities of the sintered specimens were measured according to Archimedes' principle. The crystalline phases after sintering and heat treatment were characterized by X-ray diffractometry (XRD). The x values of α-sialon phases $M_xSi_{12-(m+n)}Al_{(m+n)}O_nN_{16-n}$ were obtained from the mean values of x_a and x_c in the follow relations [15]:

$$a\,(\mathrm{nm}) = 0.775 + 0.0156x_a \quad (1)$$

$$c\,(\mathrm{nm}) = 0.562 + 0.0162x_c \quad (2)$$

Hardness (HV_{10}) and indentation fracture toughness (K_{IC}) were determined by the Vickers diamond indentation method with a 98 N load on the polished surfaces. K_{IC} was evaluated by the method of Anstis et al. [16], assuming a Young's modulus of 300 GPa.

After application of a carbon coating, both the polished surfaces etched by molten NaOH for 5 min and fracture surfaces of HP-sintered and heat-treated samples were examined using scanning electron microscope (SEM). Selected microstructures were characterized in detail by transmission electron microscopy (TEM). To characterize the grain morphology of the investigated materials, the grain dimensions were measured for over 300 grains according to several SEM micrographs. The apparent aspect ratio of each grain was determined from length/diameter.

3. Results and discussion

3.1. Densification

Near fully densified Y or Yb containing sialon compacts (see Table 2) were obtained after hot pressing at 1900 °C for 1 h, indicating that the addition of 2 wt.% extra liquid phase could effectively promote densification. However, the same α-sialon compositions (i.e. Y1010 or Yb1010) could not be densified without the incorporation of excess Y_2O_3 or Yb_2O_3, and their relative densities are only 70% and 65%, respectively, after hot-pressed at 1900 °C for 1 h [17]. For Y- or Yb-doped α-sialons, the tendency to form α-sialon grains is very strong due to the small cation size, the liquid phase is gradually exhausted with the formation of α phase at intermediate stages of densification [18]; further densification at final stage becomes very difficult. Therefore, for Y- or Yb-α-sialons with low x values (such as in this study, $x = 1/3$), it is necessary to add more additives to ensure the formation of a fully dense product. Hence, the Yb, Y and Yb/Y1010E2 were the main investigated materials in our work.

3.2. Phase analysis

Phase compositions and lattice parameters of the investigated α-sialons after hot pressing and post-heat treatment are shown in Table 2, indicating that, as expected, only α-sialon phases exists in all the investigated specimens. None of the samples contain secondary crystalline phases as determined by XRD (Fig. 1), indicating that the cooling rate was sufficient to prevent any crystallization of the grain boundary glass-phase.

Table 2
X-ray phase assemblage, lattice parameters and relatively density of the investigated sialons after HP-sintering and post-heat treatment

Sample	Sintering condition	Phase assemblage	α-Sialon			Relative density (%)
			a (nm)	*c* (nm)	*x*	
Yb1010E2	HP1900 °C, 1 h	α-Sialon	0.7809	0.5687	0.40	99.93
Yb1010E2	HP1500 °C, 1 h/1900 °C, 1 h	α-Sialon	0.7807	0.5688	0.39	99.85
Y1010E2	HP1900 °C, 1 h	α-Sialon	0.7805	0.5684	0.37	99.96
Y1010E2	HP1500 °C, 1 h/1900 °C, 1 h	α-Sialon	0.7805	0.5683	0.37	99.90
Yb/Y1010E2	HP1900 °C, 1 h	α-Sialon	0.7810	0.5685	0.39	99.94
Yb/Y1010E2	HP1500 °C, 1 h/1900 °C, 1 h	α-Sialon	0.7808	0.5686	0.39	99.92
Yb1010E2	HP1900 °C, 1 h/HT1900 °C, 1 h	α-Sialon	0.7811	0.5689	0.41	–
Y1010E2	HP1900 °C, 1 h/HT1900 °C, 1 h	α-Sialon	0.7810	0.5687	0.40	–
Yb/Y1010E2	HP1900 °C, 1 h/HT1900 °C, 1 h	α-Sialon	0.7813	0.5687	0.41	–

Table 2 also shows that the unit cell dimension of α-sialon phase is similar in all samples, the solubility of stabilizing metal is only slightly higher in Yb1010E2 sample than that in Y1010E2 sample. Post-heat treatment at 1900 °C for 1 h has no obvious effect on the phase assemblages in any of the samples and only shows a slight increase in the unit cell volume of α-sialon phase.

3.3. Microstructures of the α-sialon ceramics

The microstructures of the investigated sialons after HP-sintering are shown in Fig. 2. Fig. 2(a) shows that the α-sialon grains in Yb1010E2 sample exhibited an equiaxed microstructure with an average grains size of about 1.3 μm. For Y1010E2 and Yb/Y1010E2 samples, the α-sialon grains generally became elongated with an average aspect ratio of 2.1–2.3, as shown in Fig. 2(c) and (e). It can also be noted that both length and width of the elongated grains in the Yb/Y1010E2 sample are greater than that in Y1010E2 sample, and the aspect ratio is near to that in Y1010E2. This observation may indicate that the type of stabilizing cation significantly affects the grain morphology of the final product.

Two-step pressing (i.e. with additional holding at 1500 °C for 1 h before heating to the sintering temperature) had no significant effect on the morphologies or aspect ratio of α-sialon grains in any of the investigated samples. This microstructure was similar to that without the low-temperature holding, as shown in Fig. 2(b), (d) and (f). Table 3 lists the average dimensions of the α-sialon grains in the investigated materials.

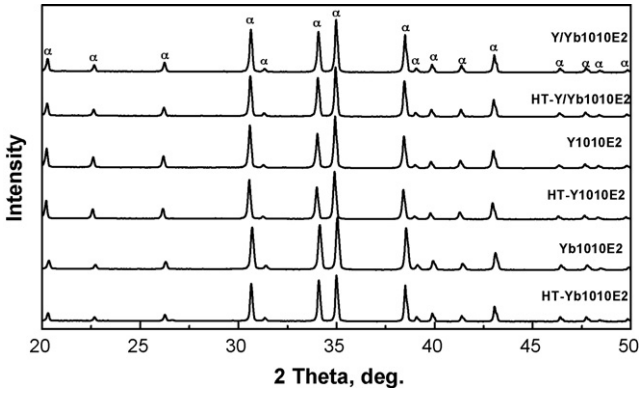

Fig. 1. XRD patterns of the investigated α-sialons after hot pressing at 1900 °C for1 h and post-heat treatment (HT) at 1900 °C for 1 h.

TEM micrographs of the sialons after HP-sintering at 1900 °C with a 1500 °C holding are shown in Fig. 3. In the Yb1010E2 sample equiaxed α-sialon grains contact closely with each other with a small amount of intergranular phase at the three-grain junctions (Fig. 3(a)). When partially or fully substituting Yb with Y as a modifying cation, elongated grains appear which are embedded into the fine-grain matrix and a trace amount of boundary phase is present at the triple-grain pockets (Fig. 3(b) and (c)). In these Y-containing samples, the contacted α-sialon grains were separated by continuous thin glassy films merging into small glassy pocket at triple points, as indicated by white arrows in Fig. 3(d). Full crystallization of the glassy films was not obtained in these areas, thin glassy boundary films also separate the adjacent α-sialon grains as indicated by circle in Fig. 3(d).

The observation that the hot-pressed Yb-doped α-sialon sample only contained equiaxed grains can be explained by the strong tendency to form α-sialon grains with few intermediate phases forming, implying that the formation and/or coarsening of α-sialon grains occurs at low temperature [18]. The gradually coarsened α-sialon grains become difficult to dissolve when they reach the final sintering temperature. It makes the anisotropic Oswald ripening mechanism of α-sialon grains hard to operate due to the lack of raw materials. Shen et al. [5,6] successfully obtained elongated grains in Yb-α-sialon by applying a very fast heating rate (SPS, 200 °C/min), indicating that controlling the nucleation rate of α-sialon phase is necessary for the formation of elongated grains. Obviously, in the present work, using two stabilizing M ions (i.e. Y + Yb) may also avoid an overabundance of nucleation sites and hence promoting the in situ formation of elongated α-sialon grains. In addition, the formation of elongated grains in our Y- and Y/Yb-doped α-sialons is also attributed to the incorporation of an excess of liquid phase, which has also been shown by other works [10,11,13].

The microstructures of Yb1010E2 and Y/Yb1010E2 samples after heat treatment at 1900 °C for 1 h are shown in Fig. 4. After heat treatment, the morphology of α-sialon grains in Yb1010E2 sialons is still equiaxed, the only difference compared with the as-sintered samples is the slightly coarser grain size (Fig. 4(a) and

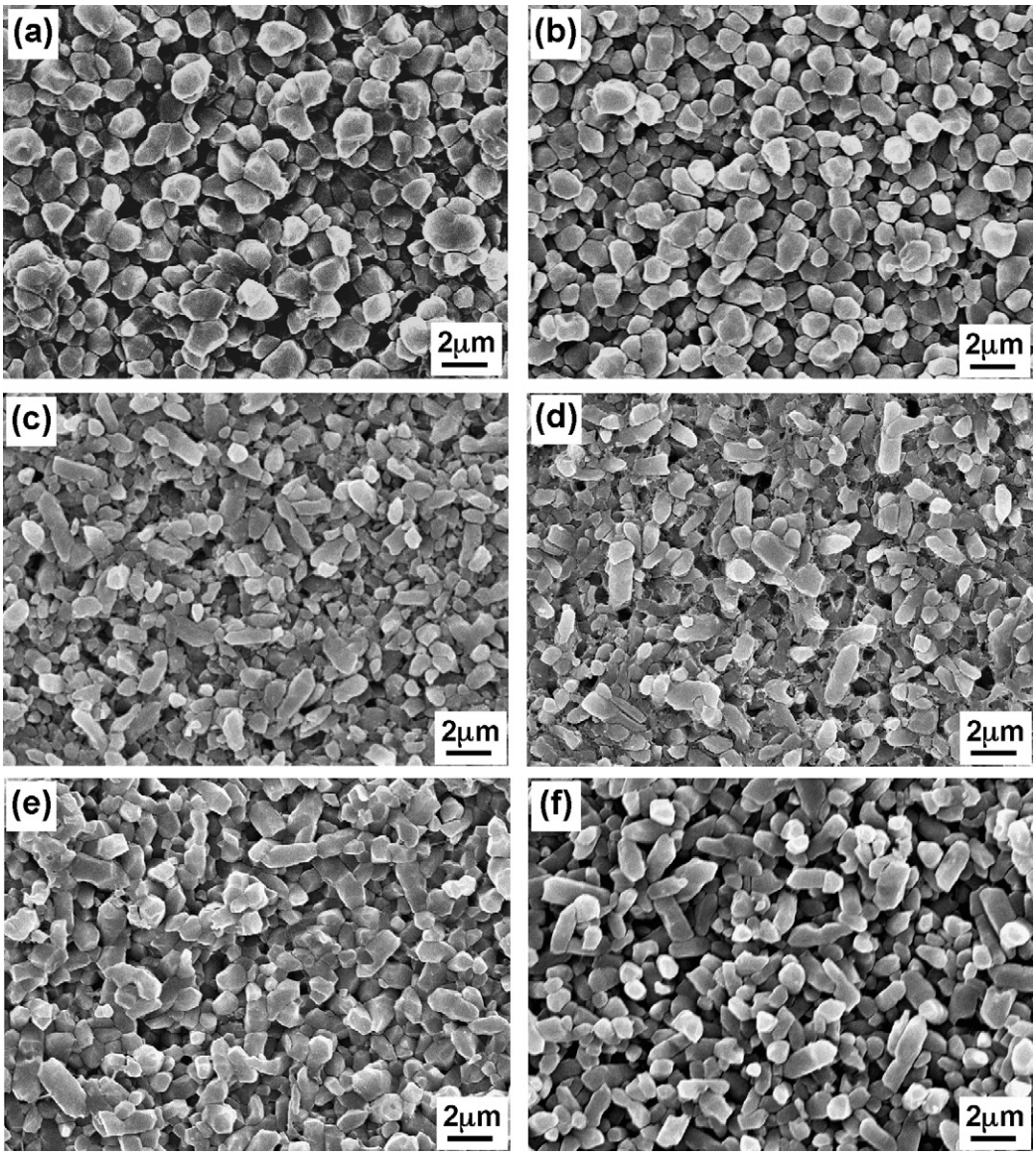

Fig. 2. SEM micrographs of investigated α-sialons after sintering: (a) Yb1010E2, HP1900 °C, 1 h; (b) Yb1010E2, HP1500 °C, 1 h/1900 °C, 1 h; (c) Y1010E2, HP1900 °C, 1 h; (d) Y1010E2, HP1500 °C, 1 h/1900 °C, 1 h; (e) Yb/Y1010E2, HP1900 °C, 1 h; (f) Yb/Y1010E2, HP1500 °C, 1 h/1900 °C, 1 h.

(b)). For Y/Yb1010E2, heat treatment at higher temperatures increases both the dimensions and anisotropy of the α-sialon grains in that they become more elongated after the heat treatment for 1 h at 1900 °C (Fig. 4(c) and (d)). The microstructural development, with post-heat treatment, in Y1010E2 samples is similar to Yb/Y1010E2 sialons. The measured values of dimensions and aspect ratio of α-sialon grains after the post-heat treatment are also listed in Table 3.

Table 3
Average grain dimensions of the investigated sialons after HP-sintering and heat treatment

Sample	Sintering condition	Length (μm)	Width (μm)	Aspect ratio
Yb1010E2	HP1900 °C, 1 h	1.33 ± 0.24	1.07 ± 0.16	1.25 ± 0.16
Yb1010E2	HP1500 °C, 1 h/1900 °C, 1 h	1.33 ± 0.22	0.98 ± 0.12	1.38 ± 0.21
Y1010E2	HP1900 °C, 1 h	1.84 ± 0.36	0.80 ± 0.10	2.30 ± 0.56
Y1010E2	HP1900 °C, 1 h/1500 °C, 1 h	1.79 ± 0.42	0.78 ± 0.14	2.27 ± 0.54
Yb/Y1010E2	HP1900 °C, 1 h	1.88 ± 0.42	0.90 ± 0.12	2.10 ± 0.42
Yb/Y1010E2	HP1500 °C, 1 h/1900 °C, 1 h	1.82 ± 0.43	0.86 ± 0.13	2.12 ± 0.47
Yb1010E2	HP1900 °C, 1 h/HT1900 °C, 1 h	1.54 ± 0.33	1.07 ± 0.19	1.45 ± 0.25
Yb1010E2	HP1500 °C, 1 h/1900 °C, 1 h/HT1900 °C, 1 h	1.66 ± 0.32	1.13 ± 0.15	1.49 ± 0.26
Yb/Y1010E2	HP1900 °C, 1 h/HT1900 °C, 1 h	2.12 ± 0.36	0.96 ± 0.15	2.25 ± 0.42
Yb/Y1010E2	HP1500 °C, 1 h/1900 °C, 1 h/HT1900 °C, 1 h	2.18 ± 0.47	0.98 ± 0.16	2.26 ± 0.48

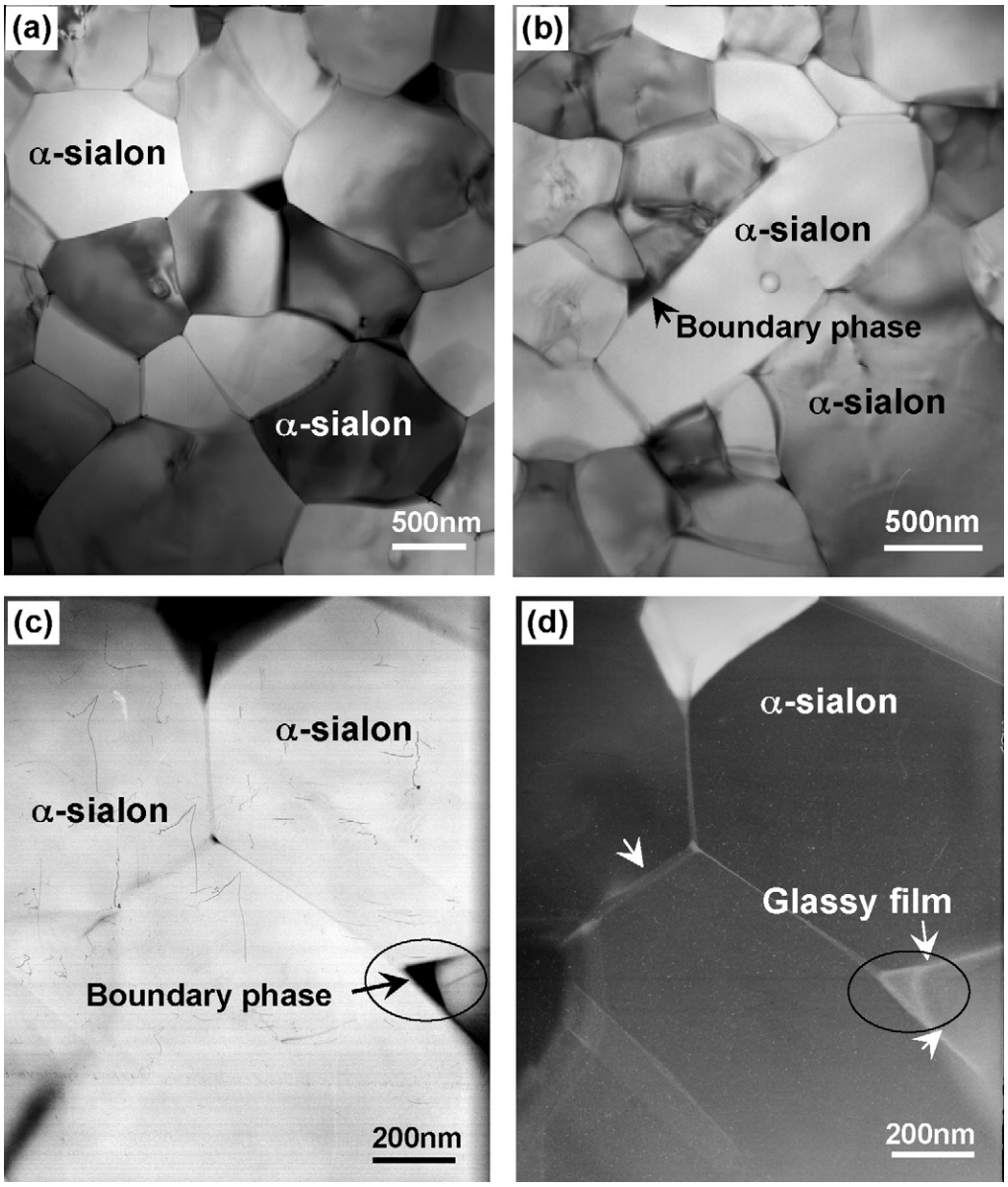

Fig. 3. TEM micrographs of investigated α-sialons after HP-sintering at 1900 °C for 1 h with a 1500 °C holding. (a)–(c) Bright field images of Yb1010E2, Y1010E2 and Yb/Y1010E2, respectively; (d) TEM dark-field image of area in (c) showing a continuous glassy phase

3.4. Mechanical properties

The Vickers hardness (HV_{10}) and indentation fracture toughness (K_{IC}) of the fabricated sialons after sintering and heat treatment are summarized in Table 4. All the samples exhibited very similar high hardness values of over 20 GPa, this was most likely because α-sialon was the only crystalline phase and all samples had a uniform high relative density. However, the influence of the type of stabilizing cation on the fracture toughness is very evident. After sintering at 1900 °C for 1 h, the fracture toughness of Yb1010 sample was 2.8 ± 0.2 MPa $m^{1/2}$. This is most probably due to its equiaxed grains morphology (shown in Fig. 2(a)), which could not effectively facilitate crack deflection and bridging during fracture. The equiaxed matrix could be seen from the Yb1010E2 fracture surface, as shown in Fig. 5(a). Both Y1010E2 and Yb/Y1010E2 samples showed significantly higher fracture toughness, their toughness values were 3.5 ± 0.2 and 3.8 ± 0.3 $MPa^{1/2}$, respectively. The increase in K_{IC} was attributed to the altered α-sialon grain morphology from equiaxed to elongated grains (as shown in Fig. 2(c) and (e)). The elongated grain microstructure would promote crack deflection, crack bridging and grain pull-out during fracture and result in a higher fracture toughness. The typical fracture surface of Yb/Y1010E2 sample is shown in Fig. 5(b). It clearly reveals the crack deflection and pulling out of elongated α-sialon grains. The slightly higher fracture toughness in Y/Yb1010E2 sample may also be due to its greater elongated grains size.

The two-step sintering process has no significant influence on the fracture toughness in all the investigated sialons, because they have very similar microstructures to those sintered without the low-temperature hold, as shown in Fig. 2. However the

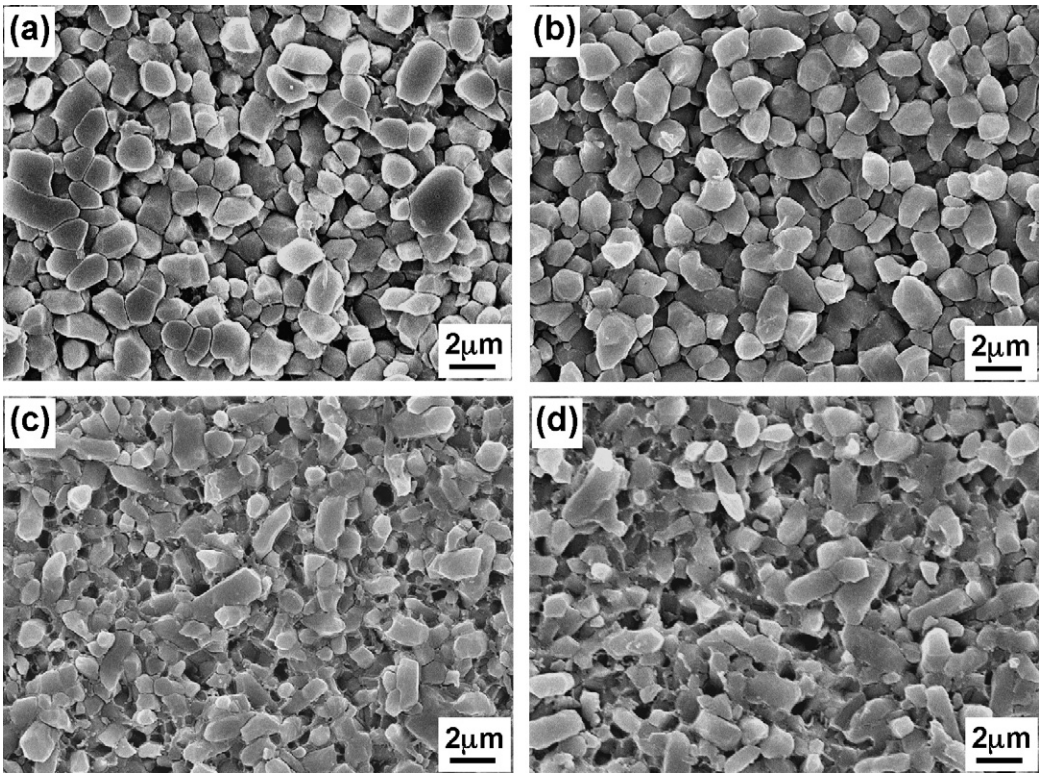

Fig. 4. SEM micrographs of investigated α-sialons after heat-treatment at 1900 °C for 1 h: (a) Yb1010E2, HP1900 °C, 1 h; (b) Yb1010E2, HP1500 °C, 1 h/1900 °C, 1 h; (c) Yb/Y1010E2, HP1900 °C, 1 h; (d) Yb/Y1010E2, HP1500 °C, 1 h/1900 °C, 1 h.

Table 4
Indentation fracture toughness (MPa $m^{1/2}$) of investigated sialons after HP-sintering and heat treatment

Sample	HP1900 °C, 1 h	HP1500 °C, 1 h/1900 °C, 1 h	HP1900 °C, 1 h/HT1900 °C, 1 h	HP1500 °C, 1 h/1900 °C, 1 h/HT1900 °C, 1 h
Yb1010E2	2.8 ± 0.2[a]	2.9 ± 0.2	3.2 ± 0.3	3.0 ± 0.2
Y1010E2	3.5 ± 0.2	3.8 ± 0.3	3.8 ± 0.2	4.0 ± 0.3
Yb/Y1010E2	3.8 ± 0.3	3.7 ± 0.2	4.1 ± 0.2	4.2 ± 0.2

[a] Hardness of all samples was about 20.7 ± 0.25 GPa.

results also showed that a post-heat treatment at 1900 °C could further increase the fracture toughness of Y1010E2 and Yb/Y1010E2 sialons. This was due to a further increase in aspect ratio of the elongated α-sialon grains during post-heat treatment of at 1900 °C (Fig. 4(c) and (d)).

4. Conclusions

1. Dense Y-, Yb- and Y/Yb-doped α-sialon ceramics can be prepared by hot pressing with the incorporation of 2 wt.% excess rare-earth oxides. The manufactured materials all

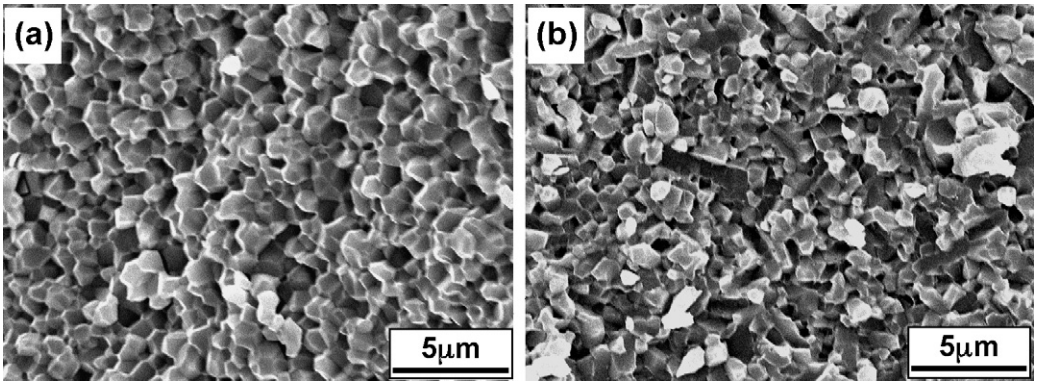

Fig. 5. SEM micrographs of fracture surfaces of (a) Yb1010E2 and (b) Yb/Y1010E2 samples sintered at 1900 °C for 1 h.

exhibited high hardness values of over 20 GPa, which are typical for α-sialons.
2. The intermediate hold during sintering has no apparently significant effect on the microstructure of all the investigated α-sialons and hence their mechanical properties.
3. The type of the stabilizing cation has a strong influence on the morphology of α-sialon grains. The Yb-doped hot-pressed α-sialon sample only contained equiaxed grains. However, for Y1010E2 and Yb/Y1010E2 samples, most α-sialon grains become elongated, with an average aspect ratio of about 2.5 using the same sintering process.
4. The formation of elongated grains increased the fracture toughness of Y- and Y/Yb-α-sialon due to the contribution of crack deflection, crack bridging and grain pull-out mechanisms.
5. The growth of elongated α-sialon grains in this work was attributed to the presence of an excess liquid phase containing Y or Y + Yb cations.

Acknowledgments

This work was supported by National Natural Science Foundation of China (Grant No. 50632020) and the Science Fund for Distinguished Young Scholars of Heilongjiang Province (Grant No. JC200603).

References

[1] G.Z. Gao, R. Metselaar, α'-Sialon ceramics: a review, Chem. Mater. 3 (2) (1991) 242–252.
[2] L.O. Nordberg, T. Ekström, G. Svensson, S. Wen, Hot-pressed SiC-whisker reinforced α-sialon composites, J. Hard Mater. 4 (1993) 121–135.
[3] L.O. Nordberg, T. Ekström, Hot-pressed $MoSi_2$-particulate-reinforced α-sialon composites, J. Am. Ceram. Soc. 78 (3) (1995) 797–800.
[4] I.W. Chen, A. Rosenflanz, A toughened sialon ceramic based on α-Si_3N_4 with a whisker-like microstructure, Nature (London) 389 (1997) 701–704.
[5] Z.J. Shen, Z. Zhao, H. Peng, M. Nygren, Formation of tough interlocking microstructure in silicon nitride ceramics by dynamic ripening, Nature (London) 417 (2002) 266–269.
[6] Z.J. Shen, H. Peng, M. Nygren, The formation of in situ reinforced microstructure in α-sialon ceramics. I. Stoichiometric oxygen-rich compositions, J. Mater. Res. 17 (2002) 336–342.
[7] I.H. Shin, D.J. Kim, Growth of elongated grains in α-SiAlON ceramics, Mater. Lett. 46 (2001) 329–333.
[8] J. Kim, A. Rosenflanz, I.W. Chen, Microstructure control of *in situ*-toughened α-SiAlON ceramics, J. Am. Ceram. Soc. 83 (7) (2000) 1819–1821.
[9] Z.H. Xie, M. Hoffman, Y.B. Chen, Microstructural tailoring and characterization of a calcium α-SiAlON composition, J. Am. Ceram. Soc. 85 (4) (2002) 812–818.
[10] S. Kurama, M. Herrmann, H. Mandal, The effect of processing conditions, amount of additives and composition on the microstructures and mechanical properties of α-SiAlON ceramics, J. Eur. Ceram. Soc. 22 (1) (2002) 109–119.
[11] H. Peng, Z.J. Shen, M. Nygren, The formation of *in situ* reinforced microstructures in α-sialon ceramics. Part II. In the presence of a liquid phase, J. Mater. Res. 17 (5) (2002) 1136–1142.
[12] C. Zhang, K. Komeya, J. Tatami, T. Meguro, Inhomogeneous grain growth and elongation of Dy-α-sialon ceramics at temperatures above 1800 °C, J. Eur. Ceram. Soc. 20 (2000) 939–944.
[13] Y. Zhang, Y.B. Cheng, Microstructural design of Ca α-sialon ceramics: effects of starting compositions and processing conditions, J. Eur. Ceram. Soc. 23 (2003) 1531–1541.
[14] W.W. Chen, W.Y. Sun, Y.W. Li, D.S. Yan, Microstructure of (Y + Sm)-α-sialon with α-sialon seeds, J. Mater. Res. 15 (10) (2000) 2223–2227.
[15] Z.J. Shen, T. Ekström, N. Nygren, Homogeneity region and thermal stability of neodymium-doped α-sialon ceramics, J. Eur. Ceram. Soc. 79 (3) (1996) 721–732.
[16] G.P. Anstis, P. Chantikul, B.R. Lawn, D.B. Marshall, A critical evaluation of indentation techniques for measuring fracture toughness, J. Am. Ceram. Soc. 64 (9) (1981) 533–538.
[17] F. Ye, M.J. Hoffmann, S. Holzer, Y. Zhou, M. Iwasa, Effect of amount of additives and post-heat treatment on the microstructure and mechanical properties of yttrium-α-sialon ceramics, J. Am. Ceram. Soc. 86 (12) (2003) 2136–2142.
[18] A. Rosenflanz, I.W. Chen, Kinetics of phase transformations in SiAlON ceramics. I. Effects of cation size, composition and temperature, J. Eur. Ceram. Soc. 19 (13–14) (1999) 2325–2335.